Analysis and Simulation of Current-Only Directional Protection Incorporating Simple Communications

Pannita Rajakrom
Department of Electronic and Electrical Engineering
University of Strathclyde
Glasgow, Scotland
Email: pannita.rajakrom@strath.ac.uk

Campbell Booth
Department of Electronic and Electrical Engineering
University of Strathclyde
Glasgow, Scotland
Email: campbell.d.booth@strath.ac.uk

Qiteng Hong
Department of Electronic and Electrical Engineering
University of Strathclyde
Glasgow, Scotland
Email: q.hong@strath.ac.uk

***Abstract*—This paper presents a review of a range of novel protection schemes and described a new fault detection method using only current measurements, based upon comparison of pre- and during-fault current angles (and communication of angular shifts between measurement locations when faults are detected). Case studies are also presented to validate the effectiveness of the proposed method. The scheme is suitable for when conventional protection is not suitable for power networks, particularly microgrid with distributed generation units and energy storage leading to bi-directional power flows during normal and fault conditions, and low- and variable fault levels. In such cases, directional relays may be necessary to provide effective protection. However, measuring both voltage and current may be expensive and the scheme highlighted here overcomes such requirements, and it is proposed that 4/5G communications or radio-based communications may provide an effective means of transferring the (low-bandwidth) data when required.**

Keywords—directional protection, microgrid, fault detection, communication, current-only relaying

I. INTRODUCTION

Relays are applied to protect the power system by tripping the part of circuit which experiences the short circuit fault. The process is straightforward when applied to conventional power system where only one direction of power flow is evident. Nowadays, the high demand of energy, together with the reduction on pollution and emissions has led to the penetration of many small renewable energy resources (RES) within power systems, particularly at the distribution level. This leads to complications and challenges associated with protection systems [1]-[2]. In microgrids, where the direction of power can be bi-directional due to the connection of the distributed generation (DG) units; the fault level depends on operation mode, type of DGs, and the number of DGs [1], [3], as well as the infeed from any grid connection (which may not always be connected and could also vary in magnitude). In addition, fault magnitude contributed by DGs can be limited and difficult to discover [1], [4]-[5] . As a result, the directional protection, which is based upon detecting the fault by using phasors derived from voltage and current are suitable to develop stability and reliability for the protection system.

However, using both voltage and current as parameters for fault detection may require massive data and heavy computation. Relays, additionally, including a voltage measurement unit (typically requiring three voltage transformers for three-phase system) are expensive [6]. Moreover, if the fault location is very close to the relay measuring point, the voltage polarization function may be compromised as the voltage is very low, leading to difficulties in determining direction/phase for such 'close-in' faults [7].

The current phase angle, with respect to some reference (e.g. voltage), will fluctuate slightly under normal conditions, depending on the nature of the loads and the power system from which the measurement is being taken. However, when faults occur, the current phase angle value will typically change considerably from its pre-fault value due to some or all of the load being short circuited and the system between the measuring point and the fault usually being mostly reactive in terms of its impedance (while loads and the power systems are normally more resistive, or controlled to be more resistive, in nature). Current-only directional scheme may represent a good choice to determine the fault current direction and therefore location when comparing multiple measurements. *Eissa* [8] presents fault detection method from the current direction measured from signals in the time-domain. However, the results of measuring from signal in time-domain still includes noise, harmonic, and possibly frequency deviations. So, the protection system may mal-operate in some cases. In addition, the paper also stresses that the direction of system power flow in normal operating condition must be known prior to faults. In [6], [9], other schemes for measuring the current direction e.g. Kalman filter, and Discrete Fourier Transform (DFT), are described for use as an alternative to processing signals using time-domain computation. However, Kalman filter is unable to remove all noise, harmonics, and may be susceptible to frequency deviations. The results from Kalman filter may be incorrect [10]. Moreover, the method in [9] demonstrates operation only for balanced faults. So, there are some problems when we use this method in real life with various types of fault. *Ukil, Deck, and Shah* [6] present fault detection using DFT-base phase angle computation. It is suitable for tackling the disturbances from resilience to noise and harmonic perspectives. However, the problem remains as described in [8], as the direction of power flow must be known in advance. In [11], a pilot protection method is described. This protection system can operate although the direction of power flow is not known. Furthermore, this system is only described for symmetrical fault cases. It may be problematic for different types of fault that are experienced in power systems (majority are single-phase). Finally, the comparison of measurements between two or more relays requires a dedicated communication system which is not mentioned in

This is a peer reviewed, accepted author manuscript of the following research contribution: Rajakrom, P., Booth, C., & Hong, Q. (2022). Analysis and simulation of current-only directional protection incorporating simple communications. In 2022 57th International Universities Power Engineering Conference (UPEC) IEEE. https://doi.org/10.1109/upec55022.2022.9917648

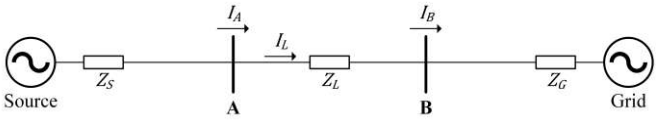

Fig. 1. Single-phase radial system diagram

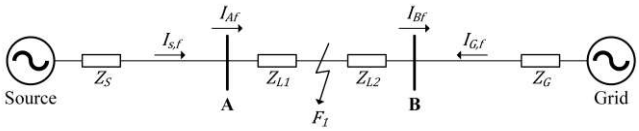

Fig. 2. During internal fault condition diagram

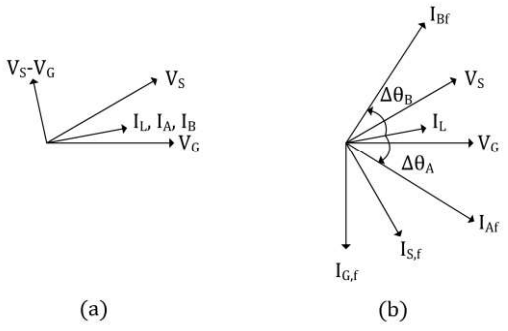

Fig. 3. Phasor diagram for (a) pre-fault current (b) current during internal fault condition when power flows from point A to B

this paper, and could hinder practical application from a cost perspective.

In this paper, the method for future microgrid protection using a communication-assisted, current-only directional scheme is explained. The proposed concept is validated using simulated case studies. The paper consists of five sections. The proposed method of microgrid protection and related communication will be analysed in Section II. In Section III, various scenarios and their results will be demonstrated. Section IV will outline future work. Finally, the overall paper will be concluded in Section V.

II. THE PROPOSED METHODOLOGY

A. Fault Detection Principle

As shown in Fig. 1, the power flows from source to grid in this example. Z_S is impedance of source, Z_G is impedance of grid, Z_L is impedance of line. V_S and V_G represent the voltage at the source and the voltage of the grid. Magnitudes and angles of current are measured by two relays at point A and point B.

According to Fig. 1, if the system operates normally, it can be stated that:

$$I_A = I_B = I_L = \frac{V_S - V_G}{Z_S + Z_L + Z_G} \tag{1}$$

when I_A and I_B are currents measured at point A and B. I_L is the line current during normal condition, and of course all are equal during normal conditions.

1) Internal Fault

Assuming fault F_1 occurs in the line between point A and B in Fig. 2.

Z_{L1} represents the impedance of line between relay A and the fault point where Z_{L2} indicates the impedance between the fault point and relay B. Relationship between Z_{L1}, Z_{L2}, and Z_L is:

$$Z_{L1} + Z_{L2} = Z_L \tag{2}$$

As can be seen in Fig. 2, during the fault condition, two fault component currents are calculated as:

$$I_{S,f} = \frac{V_S}{Z_S + Z_{L1}} \tag{3}$$

$$I_{G,f} = \frac{V_G}{Z_G + Z_{L2}} \tag{4}$$

where $I_{S,f}$ represents the fault current that is supplied from the source to the fault location (F_1), whereas $I_{G,f}$ represents the fault current that runs from the grid to the lowest potential point at the fault location (F_1)

By the superposition principle, when the fault occurs at F_1, the current flowing through the line at both ends are:

$$I_{Af} = I_A + I_{S,f} = \frac{V_S - V_G}{Z_S + Z_L + Z_G} + \frac{V_S}{Z_S + Z_{L1}} \tag{5}$$

$$I_{Bf} = I_B - I_{G,f} = \frac{V_S - V_G}{Z_S + Z_L + Z_G} - \frac{V_G}{Z_S + Z_{L2}} \tag{6}$$

where I_{Af} and I_{Bf} are the fault current that would be measured by relay A and relay B respectively. Fault impedance can be neglected due to its very small value, although in a practical application this may not be the case.

Then, the phasor diagram of currents and voltages can be drawn as shown in Fig. 3.

As presented in Fig. 3, during the fault, the fault current that relay A detects (I_{Af}) lags the load current (I_A) by certain value. In the contrary, the fault current detected by relay B (I_{Bf}) leads the load current (I_B).

Therefore, phase angle change between I_A and I_{Af} ($\Delta\theta_A$) and phase angle change between I_B and I_{Bf} ($\Delta\theta_B$) are as follows:

$$\Delta\theta_A = \theta_A - \theta_{Af} \tag{7}$$

$$\Delta\theta_B = \theta_B - \theta_{Bf} \tag{8}$$

where θ_A and θ_B are the angle of pre-fault (load current) measured at point A and B, θ_{Af} and θ_{Bf} are the angle of current as measured during fault conditions.

As illustrated in Fig. 3, because of the lagging angle of I_{Af} compared with I_A, the current phase angle at point A measured from pre-fault to during-fault is "rotated" in a clockwise (CW) direction while the current phase angle at point B is counterclockwise (CCW), or it can be estimated that the value of phase change between pre-fault current and

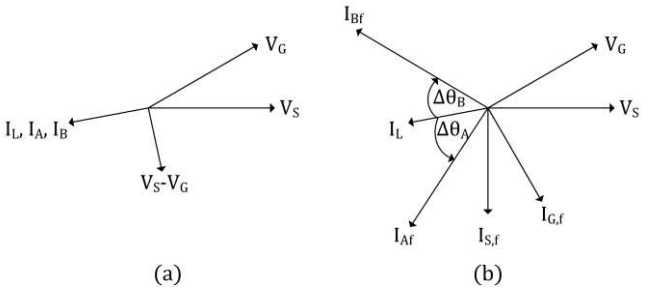

Fig. 4. Phasor diagram for (a) pre-fault current (b) current during internal fault condition when power flows from point B to A

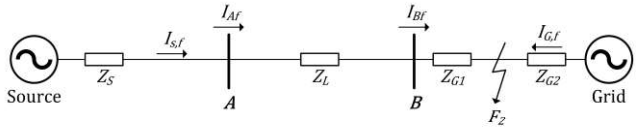

Fig. 5. During external fault condition diragram

during-fault current at point A to be positive ($0° \leq \Delta\theta_A < 180°$) while the phase angle change at B will be negative ($-180° \leq \Delta\theta_B < 0°$) since I_{Bf} leads I_B. It can be thus assumed that the rotation of phase angle change at point A and B is opposite in case of internal faults between the relay measuring points.

Conversely, if the direction of pre-fault power flow of the system in Fig. 1 runs from grid to source (loads are not shown but would be connected in practice), the phasor diagram of the system when the internal fault occurs can then be drawn as follows in Fig. 4.

As seen from Fig. 4, although the power is flown from B to A, the rotation of phase angle change calculated at point A and *B* is still the opposite. So, it can be concluded that in the case of internal faults, the opposite rotation of angle change measured at each line end always exists, regardless of the direction of power flows prior to the fault.

2) External Fault

As seen in Fig. 5, the fault in this case (F_2) occurs between point B and the grid and is therefore external to the protection protecting line A-B.

During fault conditions, the value of the fault impedance is ignored. Z_G is divided into 2 parts as follow:

$$Z_G = Z_{G1} + Z_{G2} \tag{9}$$

Two fault component currents are shown as:

$$I_{S,f} = \frac{V_S}{Z_S + Z_L + Z_{G1}} \tag{10}$$

$$I_{G,f} = \frac{V_G}{Z_{G2}} \tag{11}$$

As with the case of the internal fault illustrated in Fig. 2, $I_{S,f}$ is the fault current flowing from the source to the lowest potential point at the fault location (F_2), while $I_{G,f}$ represents the fault current that is supplied from the grid to the fault location (F_2)

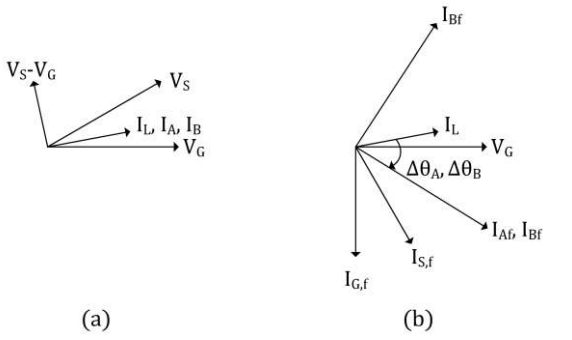

Fig. 6. Phasor diagram for (a) pre-fault (b) during external fault condition when power flows from point A to B

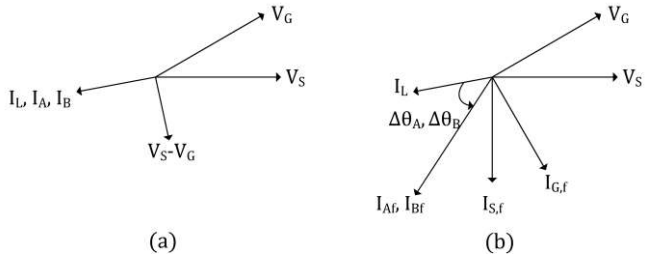

Fig. 7. Phasor diagram for (a) pre-fault current (b) current during external fault condition when power flows from point B to A

From the superposition method, the total currents flowing through each terminal of the transmission line can be calculated by using formula (1), (10) and (11):

$$I_{Af} = I_A + I_{S,f} = \frac{V_S - V_G}{Z_S + Z_L + Z_G} + \frac{V_S}{Z_S + Z_L + Z_{G1}} \tag{12}$$

$$I_{Bf} = I_B + I_{S,f} = \frac{V_S - V_G}{Z_S + Z_L + Z_G} + \frac{V_S}{Z_S + Z_L + Z_{G1}} \tag{13}$$

The phasor diagram for voltages and currents before and during the faults are as depicted in Fig. 6.

When the fault occurs as explained in Fig. 5, the fault current measured by relay A (I_{Af}) lags the load current (I_A) by a certain value. Simultaneously, the fault current measured by relay B (I_{Bf}) also lags the load current (I_B).

Thus, the phase angle change between I_A and I_{Af} ($\Delta\theta_A$) and phase angle change between I_B and I_{Bf} ($\Delta\theta_B$) are calculated using (7) and (8).

As illustrated in Fig. 6, because of the lagging of I_{Af} comparing with I_A, the change of current phase angle, measured at point A, from pre-fault to during-fault is clockwise while the same exists at point B (I_{Bf} lags I_B). Or it can be estimated that the rotation of phase angle change between pre- and during-fault current at point A and the value of phase angle change at point B are both positive ($0° \leq \Delta\theta_A, \Delta\theta_B < 180°$). It can be thus assumed that the rotation of phase angle change at point A and B are same, therefore indicating the presence of an external fault.

Moreover, if the direction of power flow of the system in Fig. 1 runs from grid to source, then the phasor diagram of the system during the external fault condition can be indicated as follows in Fig. 7.

Fig. 8. The flow chart for fault detection method

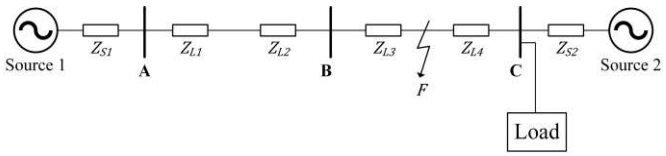

Fig. 9. Diagram of fault detection case studies

As seen from Fig. 7, although the power is flowing from B to A, the rotation of the phase angle change calculated at point A and B are still alike. So, it can be concluded that in the case of external faults, the similar rotation of phase angle change measure at each line end always exists, regardless of the direction of pre-fault power flows.

Therefore, the fault detection method can be summarized as shown in Fig. 8.

The method described above requires the phase comparison between pre-fault and during-fault currents, therefore a "moving window" and memory of prior measurements is required. This may need a certain time duration to determine the phasor quantities and calculated any shifts in relative angles. So, the effectiveness of stability and reliability of the directional relay based on the current-only depends heavily on the algorithm to quantify the current phasor. There are several methods to calculate the voltage and current phasor in the system, e.g., measuring signal directly, and Kalman filter [9]. However, the scheme used by most researchers is Discrete Fourier Transform (DFT), as it is suited for detecting the total harmonic and reduces complicate calculation steps. Although this may require some time, at distribution/microgrid levels, fault clearance times of 100s of ms are acceptable.

Another challenge of applying this principle is with respect to the various types of faults that occur in practical systems. The explanation of the above system can be applied only for the balanced fault where the system can be represented by single-phase. However, for a three-phase system, the types of fault that may occur are various and uncertain. These include single-line-to-ground, line-to-line, line-to-line-to-ground, and three-phase fault. Different fault types require different calculation methods. However, the positive sequence components of the current occur with all fault types, so it can be used for the protection against all fault types.

B. Communication System

To identify whether the fault is occurring on the protected line or not, a communication system would be used to exchange information between the relay located at the line ends, but this is only required during faults. Instead of continually sending current quantities from each end for continual comparison to determine whether any fault is 'Internal' or 'External', only the angular changes from pre- to during-fault conditions as measured by each relay are exchanged. The magnitude of the angle change could be exchanged, or a simple '0' if the angular change is clockwise or a '1' otherwise [12]. The relay will then decide upon fault location according to the following criteria: if the polarity change is the same then the fault is 'External'; if the changes are in opposite directions, it is then concluded that there is an 'Internal' fault. As already mentioned, the relays do not need to exchange these data continuously. The exchange takes place only when the fault occurs. In the event of loss of communications, a more simple but less effective graded overcurrent function could be used as backup.

Candidate low-cost communication schemes such as commercial CDMA450, GPRS or 5G could be used for this system, and future work will focus on establishing the candidate technologies and demonstrating their operation in a laboratory-based prototype using real time simulation and hardware-in-the-loop using the facilities available at the University of Strathclyde.

III. STUDY SCENARIOS

To validate the methodology described in Section II, the three-phase 11 kV system with two sources and 1 MW load as shown in Fig. 9 is characterised using MATLAB/Simulink simulation. The Fourier block diagram is used for computing voltage and current phase angles. A sequence analyser is used for calculating the magnitude and phase angle of positive sequence components. Each source has resistive and inductive impedance. Also, line impedance is represented using typical resistive and inductive parameters and the length between point A and point B is 3 kilometres, as is the length of line between point B and point C. All types of fault can be simulated at various points on the system.

Under normal operating condition, the direction of system power flow runs from source 1 to source 2, however, the reverse power flow is also simulated to confirm the applicability of the proposed algorithm.

The parameters are defined as:

- Short circuit level of source 1 = 476.31 MVA
- Voltage phase angle of source 1 = 0°
- Short circuit level of source 2 = 476.31 MVA
- Voltage phase angle of source 2 = 0°

- *X/R* ratio = 5
- Frequency = 50 Hz
- Line resistance [13] = 0.0669 ohm/km
- Line reactance [13] = 0.1053 ohm/km

This model is used to vary fault locations for both internal and external faults. The fault location is set by 10%, 20%, 30%, 40%, 50% of the length between point B and point C.

A. Power Flows from Source 1 to Source 2

Following simulating a model that is used to represent a phase-A-to-ground fault case (A-G fault), the pre-fault and during-fault positive sequence components of the current phase angles measured at point A, B, and C are shown in Fig. 10.

According to Fig. 10, the phase angle change of the positive sequence component current from normal operation to fault conditions at points A, B, and C can be calculated by using formulae (7) and (8). By shifting the fault location along the line BC, the value of $\Delta\theta_A$ varies between 74.438° and 76.149°, the value of $\Delta\theta_B$ is between 74.433° and 76.149°, and the value of $\Delta\theta_C$ is between -102.507° and -99.626°.

Since the during-fault currents lags when compared to the corresponding pre-fault values, the phase angle change of the current between normal operation and fault condition at point A ($\Delta\theta_A$) is positive ($0° \leq \Delta\theta_A < 180°$) or CW rotation. Similarly, the angular change calculated at point B is also positive. However, $\Delta\theta_C$ is negative ($-180° \leq \Delta\theta_C < 0°$) or CCW because the during-fault current leads pre-fault current.

Since the rotation of angular change calculated by relay A and B is identical, while those at B and C are opposite in rotational direction, it can thus be concluded that the A-G fault is occurring between points B and C, and the protection relays could trip the appropriate circuit breakers to clear the fault.

Table I shows the maximum and minimum phase angle change from simulation in Fig. 9 when varying fault types and locations. The results indicate the similar rotation of phase angle changes, even although the fault types are changed.

B. Power Flows from Source 2 to Source 1

As the power flows from source 2 to source 1, the rotational changes of the pre- and during-fault current angles measured at point A, B and C are shown in Table II. The direction of $\Delta\theta_A$ is counterclockwise, the same as the direction of $\Delta\theta_B$, whereas the direction of $\Delta\theta_C$ is clockwise. The same conclusion can be made although the power flow is reversed. The polarity of $\Delta\theta_A$ and $\Delta\theta_B$ is identical but opposite to $\Delta\theta_C$, so the fault is deemed to be occurring between points B and C.

IV. FUTURE WORK

This paper has focused on a fault detection methodology and various case studies using simulation to validate the performance of the scheme. As there is comparison of at least two current phase angles from each relay, data transmission of current phase angle change is required and this requires communication system to support this protection scheme [14].

In addition, although the power system in this paper is a conventional system, modern and future systems will be more complicated, especially in the case of microgrids with Distributed Generators (DGs) and energy storage. This may affect fault current magnitudes, directions and angles in the system. Researchers state that DG with inverters may limit fault levels to be around 1.5 times rated current magnitude in islanded mode [1]-[2], [4]-[5]. Accordingly, all of these factors may increase the difficulty of accurate fault detection and location, and alternative protection solutions will most likely be required in the future. The next and important phases of the research reported in this paper is to analyse the proposed protection methodology for microgrids incorporating DGs and energy storage, and validate its operation simulation in both grid-connected and islanded mode. Other work will evaluate and demonstrate communications technologies, evaluate performance in back-up mode and where communications is lost, and investigate practical implementation using hardware-in-the-loop prototypes using real time simulation capabilities available at the University of Strathclyde.

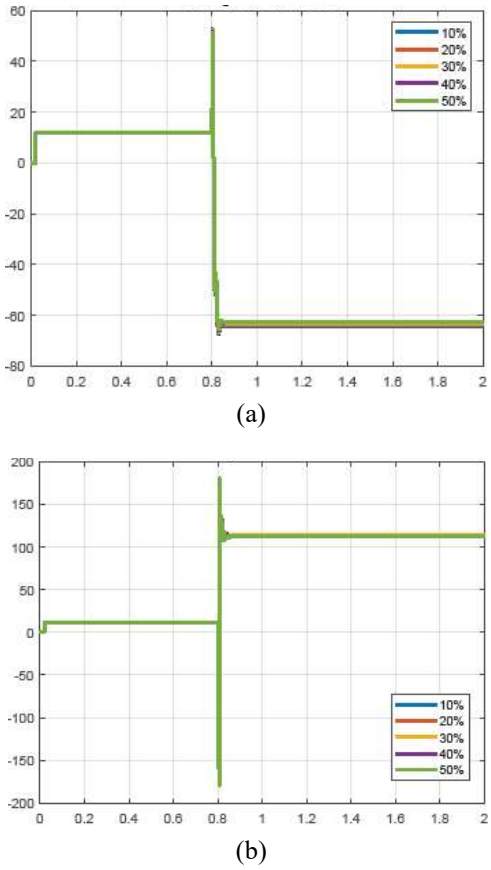

Fig. 10. Pre- and during-fault positive sequence component of current phase angle during A-G fault, measured at (a) point A and point B (b) point C

V. CONCLUSION

This paper has presented a current-only directional protection algorithm which operates by exchanging and comparing the phase angle changes measured by multiple relays, without any voltage measurement. Compared with conventional differential and directional protection schemes, this proposed method may be simpler and potentially more effective and efficient. Moreover, the scheme is appropriate for networks with no voltage measurements, which reduces cost, or could be used as a back-up protection system in other networks, for example when voltage measurement devices

TABLE I. PRE- AND DURING-FAULT POSITIVE SEQUENCE OF CURRENT PHASE ANGLE MEEASURED AT POINT A, B, AND C WHEN POWER FLOWS FROM SOURCE 1 TO SOURCE 2

Type of fault	Relay	Positive Sequence of Current Phase Angle (Degree)		Phase Angle Change (Degree)	
		Max. Value	*Min. Value*	*Max. Value*	*Min. Value*
Normal Cond.	A	11.957	11.957	-	-
	B	11.957	11.957	-	-
	C	11.957	11.957	-	-
B-G	A	-62.476	-64.192	76.149	74.433
	B	-62.476	-64.192	76.149	74.433
	C	114.46	111.58	-102.507	-99.626
C-G	A	-62.476	-64.193	76.149	74.433
	B	-62.476	-64.193	76.149	74.433
	C	114.463	111.582	-99.626	-102.507
A-B	A	-64.388	-65.919	77.876	76.344
	B	-64.388	-65.919	77.876	76.344
	C	112.859	109.793	-97.837	-100.903
A-C	A	-64.388	-65.920	77.876	76.344
	B	-64.388	-65.920	77.876	76.344
	C	112.859	109.793	-97.837	-100.903
B-C	A	-64.388	-65.920	77.876	76.345
	B	-64.388	-65.920	77.876	76.345
	C	112.859	109.793	-97.837	-100.903
A-B-G	A	-63.542	-65.148	77.105	75.498
	B	-63.542	-65.148	77.105	75.498
	C	113.690	110.699	-98.743	-101.734
A-C-G	A	-63.542	-65.148	77.105	75.498
	B	-63.542	-65.148	77.105	75.498
	C	113.690	110.699	-98.743	-101.735
B-C-G	A	-63.542	-65.148	77.105	75.498
	B	-63.542	-65.148	77.105	75.498
	C	113.690	110.699	-98.743	-101.734
3-Phase	A	-64.465	-65.983	77.940	76.422
	B	-64.465	-65.983	77.940	76.422
	C	112.915	109.836	-98.743	-101.734

TABLE II. PRE- AND DURING-FAULT POSITIVE SEQUENCE OF CURRENT PHASE ANGLE MEEASURED AT POINT A, B, AND C WHEN POWER FLOWS FROM SOURCE 2 TO SOURCE 1

Type of fault	Relay	Positive Sequence of Current Phase Angle (Degree)		Phase Angle Change (Degree)	
		Max. Value	*Min. Value*	*Max. Value*	*Min. Value*
Normal Cond.	A	-168.042	-168.042	-	-
	B	-168.042	-168.042	-	-
	C	-168.042	-168.042	-	-
A-G	A	-62.869	-64.522	-103.520	-105.173
	B	-62.869	-64.522	-103.520	-105.173
	C	114.759	111.804	80.154	77.199
B-G	A	-62.869	-64.522	-103.520	-105.173
	B	-62.869	-64.522	-103.520	-105.173
	C	114.759	111.804	80.154	77.199
C-G	A	-62.869	-64.522	-103.520	-105.173
	B	-62.869	-64.522	-103.520	-105.173
	C	114.758	111.804	80.154	77.200
A-B	A	-64.624	-66.119	-101.923	-103.418
	B	-64.624	-66.119	-101.923	-103.418
	C	113.038	109.927	82.031	78.920
A-C	A	-64.624	-66.119	-101.923	-103.418
	B	-64.624	-66.119	-101.923	-103.418
	C	113.038	109.927	82.031	78.920
B-C	A	-64.624	-66.119	-101.923	-103.418
	B	-64.624	-66.119	-101.923	-103.418
	C	113.038	109.927	82.031	78.920
A-B-G	A	-63.701	-65.285	-102.757	-104.341
	B	-63.701	-65.285	-102.757	-104.341
	C	113.813	110.790	81.168	78.145
A-C-G	A	-63.701	-65.285	-102.757	-104.341
	B	-63.701	-65.285	-102.757	-104.341
	C	113.813	110.790	81.168	78.145
B-C-G	A	-63.701	-65.285	-102.757	-104.341
	B	-63.701	-65.285	-102.757	-104.341
	C	113.813	110.790	81.168	78.145
3-Phase	A	-64.546	-66.056	-101.987	-103.496
	B	-64.546	-66.056	-101.987	-103.496
	C	112.982	109.884	82.074	78.976

fail. The case studies demonstrate the feasibility of this scheme. However, the communication network used for protection support and the algorithm for microgrid with DGs and energy storages require further investigation and study, and this is outlined as future work.

REFERENCES

[1] B. J. Brearley and R. R. Prabu, "A Review on Issues and Approaches for Microgrid Protection," *Renewable & sustainable energy reviews,* vol. 67, pp. 988-997, 2017.

[2] C. Chandraratne, T. N. Ramasamy, T. Logenthiran, and G. Panda, "Adaptive Protection for Microgrid with Distributed Energy Resources," *Electronics (Basel),* vol. 9, no. 11, pp. 1-14, 2020.

[3] T. S. Ustun, C. Ozansoy, and A. Zayegh, "A Microgrid Protection System with Central Protection Unit and Extensive Communication," in *10th International Conference on Environment and Electrical Engineering*, Rome, Italy, 2011.

[4] C. Liang, M. E. Khodayar, and M. Shahidehpour, "Adaptive Protection System for Microgrids: Protection Practices of a Functional Microgrid System," *IEEE Electrification Magazine,* vol. 2, no. 1, pp. 66-80, 2014.

[5] M. A. U. Khan, Q. Hong, A. Dyśko, and C. Booth, "Review and Evaluation of Protection Issues and Solutions for Future Distribution Networks," in *54th International Universities Power Engineering Conference (UPEC)*, Bucharest, Romania, 2019.

[6] A. Ukil, B. Deck, and V. H. Shah, "Current-Only Directional Overcurrent Relay," *IEEE Sensors Journal,* vol. 11, no. 6, pp. 1403-1404, 2011.

[7] W. A. Elmore, *Protective Relaying: Theory and Applications*. Baton Rouge: CRC Press, 2004.

[8] M. M. Eissa, "Evaluation of a New Current Directional Protection Technique Using Field Data," *IEEE Transactions on Power Delivery,* vol. 20, no. 2, pp. 566-572, 2005.

[9] A. K. Pradhan, A. Routray, and S. M. Gudipalli, "Fault Direction Estimation in Radial Distribution System Using Phase Change in Sequence Current," *IEEE Transactions on Power Delivery,* vol. 22, no. 4, pp. 2065-2071, Oct 2007.

[10] A. Ukil, B. Deck, and V. H. Shah, "Current-Only Directional Overcurrent Protection for Distribution Automation: Challenges and Solutions," *IEEE Transactions on Smart Grid,* vol. 3, no. 4, pp. 1687-1694, 2012.

[11] C. Zhou, G. Zou, J. Yang, and X. Lu, "Principle of Pilot Protection based on Positive Sequence Fault Component in Distribution Networks with Inverter-interfaced Distributed Generators," in *2019 IEEE PES GTD Grand International Conference and Exposition Asia (GTD Asia)*, Bangkok, Thailand, 2019, pp. 998-1003.

[12] J. Nsengiyaremye, B. C. Pal, and M. M. Begovic, "Microgrid Protection Using Low-Cost Communication Systems," *IEEE Transactions on Power Delivery,* vol. 35, no. 4, pp. 2011-2020, 2020.

[13] Metropolitan Electricity Authority, *Physical & Electrical Characteristics of 12/20 (24) kV XLPE Insulated Copper Cable*, internal MEA report, Bangkok, Thailand, 2020, Unpublished.

[14] J. Ciufo and A. Cooperberg, *Power System Protection: Fundamentals and Applications* (IEEE Press Series on Power and Energy Systems). Newark: John Wiley & Sons, Incorporated, 2021.